

Subplantation Model for Film Growth From Hyperthermal Species: Application to Diamond

Y. Lifshitz,^(a) S. R. Kasi, and J. W. Rabalais

Department of Chemistry, University of Houston, Houston, Texas 77204-5641

(Received 1 August 1988)

A model for film growth from hyperthermal ($\approx 1-10^3$ eV) species impinging on substrates is proposed. The process includes subsurface implantation, energy loss, preferential displacement of atoms with low displacement energies (E_d) leaving high E_d atoms undisplaced, and sputtering of substrate material. Epitaxial growth and preferred orientation result from the angular dependence of the E_d and the host *mold* effect. The model, supported by ion-trajectory calculations and experimental data, is applied to diamond film formation from C^+ ions.

PACS numbers: 68.55.Bd

Hyperthermal species [energies (E) $\approx 1-10^3$ eV] are used extensively in film deposition technology in the form of plasma and ion-beam techniques for fabrication of films, including semiconductors, metals, and ceramics.¹⁻⁴ The unique advantages of using such species are (i) epitaxial growth of crystalline films at low substrate temperatures^{5,6} and (ii) production of hard, dense, and sometimes metastable materials.^{2,3} It has been stated¹ that "this collection of structural effects does not yet provide a basis for fundamental understanding and control of film structures . . ." The use of thermal-evaporation surface-deposition mechanisms^{5,7} or other surface notations in the context of hyperthermal particle deposition is inappropriate and leads to confusion. The currently used mechanisms such as preferential sputtering³ and thermal spikes² do not provide satisfactory explanations for the data. This Letter describes a general model for film formation by hyperthermal species, with diamond film deposition serving as an example.

Carbon containing energetic species are used for the production of films with properties that vary between those of the two most common carbon allotropes, namely graphite and diamond.^{2,3,8,9} Aisenberg and Chabot⁹ showed that hard, transparent, insulating carbon films could be produced from a mixture of C^+ and Ar^+ ions in the energy range $50 < E < 100$ eV. Subsequently, ion and plasma deposition methods have been applied in attempts to deposit pure diamond films.^{2,3,8,9} Of special interest are works¹⁰⁻¹² which uniquely use mass-selected low-energy C^+ ion beams for deposition of pure diamond films at room temperature under UHV conditions. Very recent x-ray-diffraction results¹³ provide evidence for the epitaxial growth of a diamond (111) film on a Si(111) substrate.

The proposed model bridges the gap between surface deposition and bulk implantation. It is supported by classical trajectory simulations using the Monte Carlo program TRIM¹⁴ and by experimental surface analysis data. It is proposed that film growth from hyperthermal particles incident on a substrate progresses along the following steps.

(a) Penetration of the energetic species into subsurface layers to a depth that depends on the E and mass of the species and the nature of the target species.

(b) Stopping of the energetic species in the substrate by means of three energy-loss mechanisms: atomic displacements, phonon excitations, and electron excitations (the latter two phenomena are sometimes collectively referred to as "thermal spikes"²). These mechanisms can play a significant role in the final structure of the evolving film, depending on the energy and nature of the projectile-target system.

(c) Occupation of a site in the host matrix that serves as a "mold" for the structure of the growing film.

(d) Increase in the concentration of the penetrating species in the host matrix resulting in formation of an inclusion of a new phase and outward expansion of the substrate layer (internal subsurface growth).

(e) During early stages of film growth, the surface is composed of mainly *substrate* atoms. These substrate surface atoms are gradually sputtered and diluted by ion-mixing mechanisms until a surface consisting of only projectile species evolves.

(f) The structure of the evolving film is determined by two major effects: (1) the *mold* effect of the host matrix, i.e., the influence of a host crystalline environment on the crystallization of a collection of injected atoms, and (2) preferential displacement of atoms with low-displacement energies compared to those with high-displacement energies, resulting in formation of a rigid matrix.

(g) Epitaxial growth and/or preferred orientation of films on crystalline material is expected to result from the mold effect and the angular dependence of the displacement probability due to (1) the sharply defined incident angle of the impinging species and (2) the different E_d 's for recoil along different crystal directions.¹⁵ For example, the anisotropy of graphite results in high E_d in the basal plane ($\Delta H_{C-C} = 7.43$ eV) similar to diamond and low E_d perpendicular to the basal plane ($\Delta H_{C-C} = 0.86$ eV). This leads to experimental *average* values of 25 and 80 eV,³ for E_d of graphite and dia-

mond, respectively.

(h) The surface features of the film and the efficiency of the deposition process depend on self-sputtering by the impinging ions. Low-sputtering yields are essential for efficient deposition and must be less than unity for net film growth to occur.

The growth of films from low-energy C^+ ions provides an excellent example of the steps in the proposed model. The first point to be considered is that hyperthermal particle deposition is a subsurface phenomenon. *In situ* surface analysis of low-energy C^+ "deposition" in Fig. 1, as well as computer simulations of C^+ penetration in Fig. 2, prove that this is a shallow implantation process. Figure 1 shows the relative intensities of the *substrate* Auger-electron spectroscopy (AES) signals versus C^+ dose on three substrates. Since the escape depth of these low- E (61–92 eV) AES electrons is $\approx 4 \text{ \AA}$,¹⁶ mainly "surface" substrate atoms from the first two monolayers are detected. For "true surface" deposition conditions, the intensities of these substrate AES lines would decrease exponentially¹⁶ with carbon dose. These substrate AES intensities for C^+ deposition remain constant even at a dose of $\approx 10^{16} \text{ atoms/cm}^2$ (~ 5 monolayers), i.e., more than twice the escape depth of the substrate AES electrons. On the other hand, the escape depth of the carbon *KLL* AES electrons at 269 eV is $\approx 8 \text{ \AA}$ and the C AES intensity increases consistently during deposition. This can be explained only by penetration of C^+ ions into subsurface layers. The higher C^+ dose required for disappearance of the gold AES signal compared to the Ni and Si signals is due to the higher (40%) backscattering (BS) yield from the high-Z gold substrate relative to

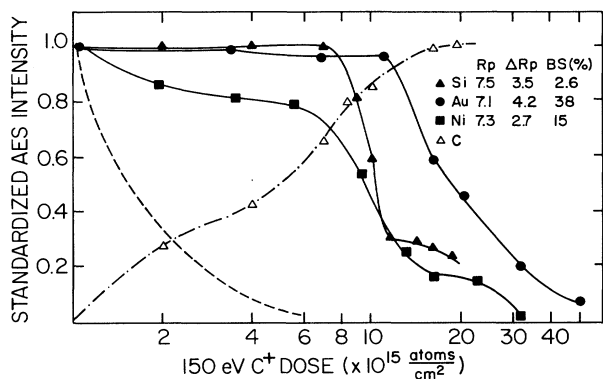


FIG. 1. Substrate AES peak intensities (solid lines) as functions of 150-eV C^+ fluence at normal incidence. Ni (61 eV), Si (92 eV), and Au (69 eV) AES transitions are used. The peak intensities are normalized to that of the clean surface. The dashed line corresponds to Si AES intensity as a function of thermally evaporated Ge dose (Ref. 16). The dashed-dotted line corresponds to the carbon *KLL* AES peak intensity specifically for the Si host. TRIM results include the following: R_p , projected range ($10^{15} \text{ atoms/cm}^2$); ΔR_p , range straggling; and BS, backscattering yield.

only 15% and 3% BS form Ni and Si, respectively. The substrate layer above the developing film is gradually removed by a combination of sputtering and ion mixing, the contributions from each being determined by the substrate mass and binding energies. For example, in the range $100 < E < 200 \text{ eV}$ the C^+ sputtering yield of Au is 0.2–0.35 but the E transferred (T) is very low, while the sputtering yields of Si and Ni are only 0.02–0.20 but the T 's are higher.

The second point is the relative significance of different E loss mechanisms for low- E particles in subsurface layers. Experimental data¹⁸ show that the sputtering yields of graphite and other carbon forms by ions such as C^+ and Ar^+ are extremely low in this E range (< 0.1 experimentally measured¹⁸ for Ar^+ and < 0.2 calculated self-sputtering yield¹⁷ for C^+ in the range 10–300 eV). Therefore, "preferential sputtering"³ of graphitic and amorphous-carbon components, leaving the diamond constituent undisturbed, cannot explain the results of diamond film growth from low-energy C^+ beams. The marked difference between the displacement energies (E_d) of diamond (80 eV) and graphite (25 eV) suggests preferential displacement of low- E_d (graphitic) atoms compared to high- E_d (diamond) atoms. Three different regimes are expected based on the E of the impinging ions as in Fig. 3. TRIM calculations (Fig. 2) confirm this hypothesis. For 25-eV C^+ , the average

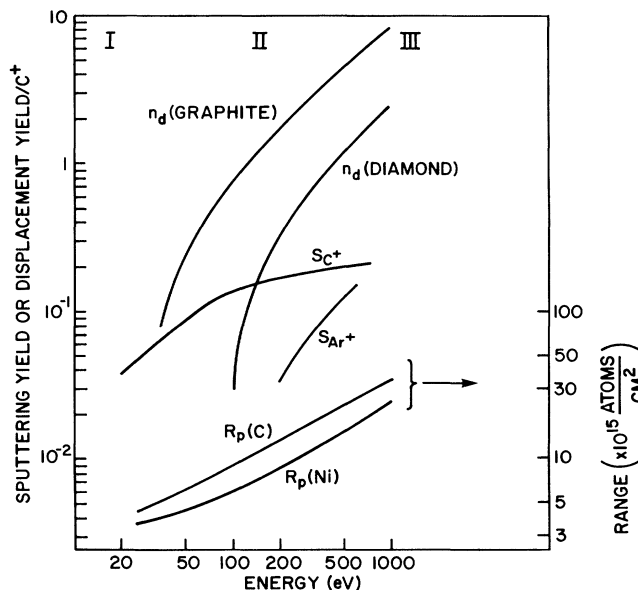


FIG. 2. TRIM calculation results: n_d , number of graphite (diamond) atoms displaced per incident C^+ ion; R_p , projected ranges of C^+ in C and Ni (atoms/cm^2); S_{C^+} , calculated carbon self-sputtering yield (Ref. 17); S_{Ar^+} , measured sputtering yield (Ref. 18) of graphite by Ar^+ . I, II, and III correspond to the E ranges of Fig. 3. Note the preferential displacement of low- E_d atoms in the 100–200-eV range where sputtering is negligible.

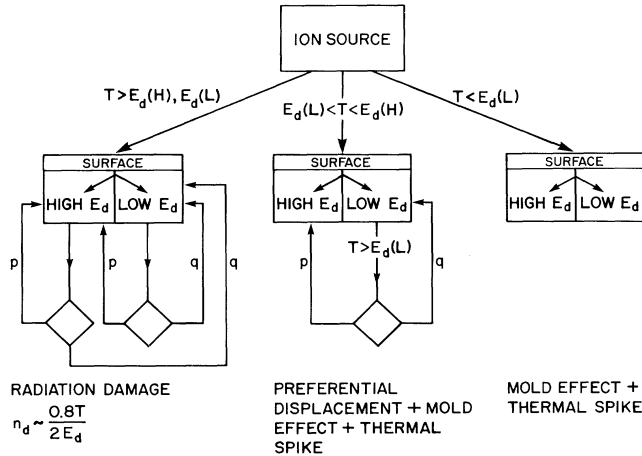


FIG. 3. Schematic illustration of dense matrix formation for three E ranges: (I) $T < E_d(L)$, only "mold effect"; (II) $E_d(L) < T < E_d(H)$, preferential displacement; and (III) $T > E_d(H)$, radiation damage and amorphization. E_d , displacement energy; H and L, high- and low- E_d atom components; T , energy transferred in collision by primary ion; n_d , number of displacements per incident primary particle; and p and q , probabilities of high- and low- E_d atomic site occupancies.

number of displacements per C^+ ion, n_d , for both graphite and diamond equals zero. For 100–200-eV C^+ , $n_d = 0.75-1.7$ for graphite and $n_d = 0.03-0.3$ for diamond. Consequently, most of the high- E_d atoms remain in their positions while the probability for each incoming ion to displace at least one to two low- E_d atoms approaches unity. At higher E , the n_d for graphitic atoms remains about 3 times larger than the n_d for diamond atoms, but both are significantly displaced, possibly resulting in graphitization or amorphization. This model assumes that the individual ion collisions and trajectories are uncorrelated, i.e., excitations induced by previous trajectories are rapidly quenched. This is a good assumption for the low-ion fluences used in these experiments. It may not be appropriate for molecular or cluster ions, e.g., C_n^+ , where the E loss processes are correlated.

TRIM calculations show that $\approx 75\%-90\%$ of the E is dissipated as phonon and electron excitations. This creates highly excited atoms localized at the collision sites which can assist in stabilization of metastable phases by providing the energy necessary for metastable site occupancy of single atoms. This is in contrast to the controversial³ concept of recrystallization of a small domain by the "thermal spike,"² due to localized melting and fast cooling ($\sim 10^{-11}$ sec). The thermal spike notation is often used as a synonym for a transient, highly excited region; however, it is difficult to treat quantitatively.

Two tests for the proposed mechanism are the dependence of film evolution on C^+ dose and E . *In situ* sur-

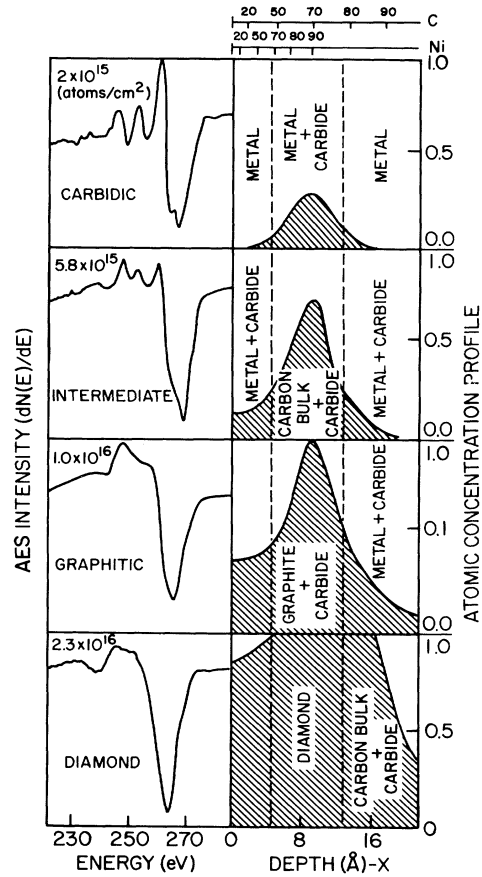


FIG. 4. Stages of subplantation growth. Left column, C *KLL* AES line shapes for different C^+ fluences for 150-eV C^+ Ni(111). Right column, subsurface entrapment of energetic carbon and buildup of carbon deposits. The top scale indicates the relative contribution to the AES intensity (%) derived from a layer of depth x (lower scale). These functions are to be compared to the Ni (AES) data of Fig. 1.

face analysis of carbon films deposited under UHV conditions shows^{11,12} that the films evolve from a carbidic, through a graphitic, to a diamond phase. This behavior corresponds to the stages of subsurface deposition at different C^+ doses as shown in Fig. 4. Our own data^{11,12} along with that of others^{3,10} show that (i) diamond, or diamondlike phases, are formed by C^+ ions in the range $\approx 50 < E < 200$ eV and (ii) the maximum film density and band gap are achieved¹⁹ for $\approx 100 < E < 200$ eV, providing a striking fit to the calculations of Fig. 2. The C^+ distribution in the different carbon phases as well as in Ni, Si, and Au "substrates" were calculated. For an increase in E from 100 to 1000 eV, the C^+ range in carbon increases from 5 ± 1 to 23 ± 9 Å, resulting in a deeper, broader implant distribution; similar qualitative results are obtained for the other substrates. This explains the previous experimental observation^{11,12} that higher C^+ doses are required to access the film growth

at higher E .

These examples illustrate the ability of this simple model to quantitatively interpret many hyperthermal ion deposition experiments. Subplantation, the suggested name for this process, is different from, but contains some features of both surface deposition and bulk implantation. Its uniqueness compared to the former is better film adhesion and the possibility of forming desirable structures at low temperature, e.g., dense, metastable, epitaxial phases.^{2-6,10,13} The advantages over the latter are shallow, narrow distribution profiles, sharp interfaces, minimal radiation damage, and crystalline films. Subplantation is a general phenomenon to which the proposed model can be applied for the formation of hard, crystalline films of different materials.^{1-3,5,6,9} A more detailed treatment will be published elsewhere.²⁰

The following conclusions are drawn. (a) "Deposition" of hyperthermal species is a shallow subsurface implantation process (suggested name, subplantation) followed by internal growth and substrate surface sputtering and dilution. (b) Evolution of rigid, dense phases occurs by a preferential displacement mechanism when the ion E is sufficient for displacement of low- E_d atoms and insufficient for displacement of high- E_d atoms. (c) Epitaxial or oriented film growth^{5,6,10,13} may be facilitated by the angular dependence of the E_d and the mold effect. (d) The subplantation model is capable of explaining many details of film growth by energetic particles from different laboratories that have previously been presented as qualitative observations without interpretations. The general nature of the model allows application to development of unique materials by proper choice of substrate, impinging species, and kinetic energy.

This material is based on work supported by the National Science Foundation under Grant No. DMR-8610597.

^(a)On sabbatical leave from Soreq NRC, Yavne 70600, Israel.

¹J. M. E. Harper *et al.*, in *Ion Bombardment Modification of Surfaces*, edited by O. Auciello and R. Kelly (Elsevier, New York, 1984), Chap. 4.

²C. Weissmantel, in *Thin Films From Free Atoms and Particles*, edited by K. J. Klabunde (Academic, Orlando, FL, 1985), Chap. 4.

³J. C. Angus, P. Koidl, and S. Domitz, in *Plasma Deposited Thin Films*, edited by J. Mort and F. Jansen (CRC, Boca Raton, FL, 1986), Chap. 4.

⁴T. Takagi, *Thin Solid Films* **92**, 1 (1982).

⁵J. E. Greene, *Solid State Technol.* **30**, 115 (1987).

⁶K. Miyake and T. Tukuyama, *Thin Solid Films* **92**, 123 (1982).

⁷G. E. Rhead, M. G. Barthes, and C. Argile, *Thin Solid Films* **82**, 201 (1981).

⁸H. Tsai and D. B. Bogi, *J. Vac. Sci. Technol. A* **5**, 3287 (1987).

⁹S. Aisenberg and R. Chabot, *J. Appl. Phys.* **42**, 2953 (1971).

¹⁰E. F. Chaikovskii, V. M. Puzikov, and A. V. Semenov, *Kristallografiya* **26**, 219 (1981) [*Sov. Phys. Crystallogr.* **26**, 122 (1981)].

¹¹S. R. Kasi, H. Kang, and J. W. Rabalais, *J. Chem. Phys.* **88**, 5914 (1988).

¹²S. R. Kasi, Y. Lifshitz, and J. W. Rabalais, *Angew. Chem.* **100**, 1245 (1988).

¹³J. L. Robertson, S. C. Moss, Y. Lifshitz, S. R. Kasi, J. W. Rabalais, G. D. Lempert, and E. Rapoport, *Science* **243**, 1047 (1989).

¹⁴J. F. Ziegler, J. P. Biersack, and U. Littmark, *The Stopping and Ranges of Ions in Matter* (Pergamon, Oxford, 1985), Vol. 1. These calculations assume a binary-collision approximation, and an amorphous target.

¹⁵G. Dearnaley *et al.*, *Ion Implantation* (North-Holland, Amsterdam, 1973), p. 155.

¹⁶L. C. Feldman and J. W. Mayer, *Fundamentals of Surface and Thin Film Analysis* (North-Holland, Amsterdam, 1986), Chap. 6.

¹⁷T. Miyazawa *et al.*, *J. Appl. Phys.* **55**, 188 (1984).

¹⁸H. H. Andersen and H. L. Bay, in *Sputtering by Particle Bombardment I*, edited by R. Behrisch (Springer-Verlag, New York, 1981), Chap. 4.

¹⁹J. Ishikawa *et al.*, *J. Appl. Phys.* **61**, 2509 (1987).

²⁰Y. Lifshitz, S. R. Kasi, and J. W. Rabalais (to be published).